JOURNAL OF CATALYSIS 127, 201–212 (1991)

Structure and Activity of Composite Oxide-Supported Iridium and Platinum Catalysts

S. SUBRAMANIAN* AND J. A. SCHWARZ†

Department of Chemical Engineering and Materials Science, Syracuse University, Syracuse, New York 13244

Received December 1, 1989; revised August 20, 1990

The objective of this study is to investigate the structure and activity of composite oxide (Al_2O_3–TiO_2 and TiO_2–Al_2O_3)-supported Pt and Ir catalysts. Two characterization techniques, temperature-programmed reduction/temperature-programmed desorption (TPRd/TPD) and ethane hydrogenolysis were used. TPRd/TPD provided information on the structure of the catalyst whereas ethane hydrogenolysis provided information on the structure and activity. The TPRd, TPD, and ethane hydrogenolysis results suggest that two processes, Al^{3+} dissolution in acidic impregnation solutions and TiO_x overlayer formation occurring in reducing environments affect the structure and activity of these catalysts. Specifically, the TPRd results indicate that the readsorbed Al^{3+} species inhibits the amount of chloride liberated during calcination; this results in an increase in the amount of hydrogen consumed during reduction. The TPD results suggest that TiO_x overlayer formation occurs in the case of composite oxides. The readsorbed Al^{3+} increases the hydrogenolysis activity of these catalysts. The intimate association of the noble metal and Al^{3+} suggests that alloys of the form Pt_3Al and IrAl may exist on the surface of the Pt and Ir catalysts. These factors have been considered and models for the structures of these catalysts have been proposed.

INTRODUCTION

In order to achieve greater understanding about how good supported metal catalysts can be prepared, more information on the structure and structure–activity relationships of catalysts is needed. It is difficult to optimize the performance of a catalyst without any information on its structure. Oxides commonly used to prepare supported metal catalysts may be classified into two categories: simple oxides and composite oxides. Composite oxides provide a way of dispersing an intrinsically low surface area carrier on a high surface area support. The number, strength, and type of acid sites can be controlled by varying their composition (*1–5*), and the catalytic properties of supported metals can be influenced by the presence of the binary oxide.

The structure, activity, and the structure–activity relationship of alumina/titania composite oxide-supported Pt and Ir catalysts are the focus of this study. Simple oxide-supported catalysts have also been studied under identical conditions to provide a basis for comparing the behavior of the composite oxide-supported catalysts. The secondary phase (minor component of the composite oxide) weight loading in the composites oxides used was relatively low, i.e., 0.87% Al_2O_3–TiO_2 and 11.4% TiO_2–Al_2O_3. The metal weight loading for the precursors was 3%. Under these conditions, based on adsorption equilibrium considerations, the maximum amount of metal that can be dispersed on the secondary phase is extremely small compared to the amount of metal that can be dispersed on the primary phase (major component of the

* Present address: Ford Motor Co., S-3068, 2162 SRL, P.O. Box 2053, Dearborn, MI 48121.

† To whom correspondence should be addressed.

0021-9517/91 $3.00

composite oxide on a weight basis). Therefore, the metal is essentially distributed on the primary phase and the secondary phase acts as a perturbation in the system.

The alumina/titania system possesses some properties of interest, alumina dissolution (*6–9*) and TiO_x overlayer formation (*10–13*). These two processes occur at different stages of catalyst preparation. While Al^{3+} dissolution and readsorption occurs during impregnation, TiO_x overlayer formation occurs in a reducing environment. The effect of these processes on the structure and activity of these catalysts has been studied using two procedures: temperature-programmed reduction/temperature-programmed desorption (TPRd/TPD) and ethane hydrogenolysis. In a typical catalyst preparation sequence, reduction is the last step that leads to the formation of the finished catalyst. In order to follow the changes occurring in these systems during reduction, temperature-programmed reduction, a dynamic characterization technique, was used. Since investigation of the structure, activity, and the structure–activity relationship is of importance here, ethane hydrogenolysis, a structure-sensitive reaction, was chosen as a test reaction. (The rate depends on the dispersion of the catalyst when the reaction under consideration is structure sensitive). While TPRd/TPD provides information on the structure of the precursor/catalyst, the ethane hydrogenolysis test reaction provides information on both the structure and the activity of the catalyst. Suppressed hydrogenolysis activity appears to be a general feature of strong metal-support interactions (SMSI) catalysts, where TiO_x overlayer formation can occur (*14, 15*). The hydrogenolysis activities of Pt and Ir on TiO_2 are approximately an order of magnitude lower than those of Pt and Ir supported on Al_2O_3.

The TPRd results indicate that readsorbed Al^{3+} inhibits the amount of chloride (resulting from the use of chloroplatinic and chloroiridic acids to prepare the precursors) liberated during calcination. The TPD results suggest that TiO_x overlayer formation occurs in the case of composite oxides. Readsorbed Al^{3+} increases the activity of Pt and Ir catalysts in the hydrogenolysis reaction; the effects are more pronounced in the case of Ir. The ethane hydrogenolysis and TPRd results suggest that alloys of the form Pt_3Al or IrAl may exist on the surface of Pt and Ir catalysts. These observations have been collectively used to propose models for the structure of the calcined precursors and finished catalysts.

EXPERIMENTAL

Preparation of Precursors

Alumina (American Cyanamid, BET area 195 m^2/g, pore volume 0.5 cm^3/g), titania (Degussa Corp., BET area 50 m^2/g, nonporous), 11.4% TiO_2–Al_2O_3, and 0.87% Al_2O_3–TiO_2 were used as supports. The procedure for preparing the composite oxides was identical to that used by Subramanian *et al.* (*16*). The thermal treatment and the particle size of all the oxides used were maintained uniform: 823 K calcination and a 40- to 80-mesh (0.225 mm) particle size.

The reagents, chloroplatinic acid and chloroiridic acid, were obtained from Johnson Matthey. Required amounts of these solids were dissolved in air-saturated double distilled water (pH = 5.6). One gram of oxide was contacted with 0.5 cm^3 of these impregnation solutions to attain a 3% metal weight loading. The precursors were dried overnight at room temperature under darkness. The precursors were further dried in air at 423 K for a period of 1 h. The precursors were calcined in air at 673 K for 4 h. These are called "Set I" precursors.

Another class of Ir/TiO_2 precursors was prepared in which Al^{3+} ions were introduced into the metal system in the form of aluminum nitrate, $Al(NO_3)_3 \cdot 9H_2O$ (J. T. Baker and Co., Analytical Grade Reagent). Here, the desired quantity of aluminum nitrate was dissolved in the Ir impregnation solution, and the resulting solution was used

to impregnate TiO_2. The resulting entities were dried and calcined. These are referred to as "Set II" precursors.

Temperature-Programmed Reduction and Temperature-Programmed Desorption

The TPRd/TPD apparatus consists of three sections: (i) The gas delivery and purification system, (ii) reactor assembly, and (iii) a thermal conductivity detector (TCD) to measure the difference in the concentration of the gas entering and leaving the reactor. Further details can be found elsewhere (*17*).

The procedures, some of which have been described before (*17*), consist of

(1) Dehydration.

(2) Room temperature reduction.

(3) First temperature-programmed reduction.

(4) First temperature-programmed desorption.

(5) Second TPRd.

This step was necessary in order to perform the second TPD step. Steps 5 and 6 are especially useful in the case of TiO_2-supported precursors. Progressive introduction of SMSI behavior (suppressed H_2 chemisorption) can be verified using steps 5 and 6.

(6) Second TPD: Step 4 was repeated.

Ethane Hydrogenolysis

The reaction unit is schematically represented in Fig. 1. The setup consists of three sections: (i) gas delivery system with facilities for mixing gases, (ii) reactor assembly, and (iii) gas chromatograph (GC) to assess the concentrations of the reactants and products.

(*1*) *Gas delivery system.* Ultra high purity (UHP) grade Ar, He, and 8.5% H_2/Ar, CP Grade C_2H_6, and Research Grade CH_4 were obtained from the Linde Division of Union Carbide Corporation. The gases were passed through Drierite to remove traces of water vapor that may be present. The H_2/Ar mixture was purified further by passing it through an oxy-sorb deoxidizer. The gases were mixed by passing them through cylindrical vessels (1-in O.D and 3-in height). These vessels were provided with three perforated plates in order to generate turbulence. The inlet nozzles were also designed to provide a swirling motion. The gas flow rates were controlled with Tylan controllers (Model FC-260), and were used to control the partial pressure of the reactants at desired levels.

(*2*) *Reactor assembly.* A differential reactor was used in this study. The reactor assembly and heating arrangements used for the reaction unit were identical to those used for TPRd/TPD experiments (*17*).

(*3*) *Gas chromatograph.* An Antek 3000 gas chromatograph was used in conjunction with a Carbosieve II (Supelco Inc.) packed column to determine the concentrations of the products and reactants. The temperature of the column and detector filaments were controlled at 488 and 323 K, respectively. A 200-mA bridge current was used. The products and reactants were periodically sampled using an on-line sampling loop (2 cm^3) in conjunction with a six-way valve. The voltage signal from the GC was monitored on an Esterline Angus (Model SS-260F) chart recorder.

The reaction conditions and procedures used are outlined below:

(*1*) *Dehydration.* A sample of 100 mg was flushed with Ar at a flow rate of 100 cm^3/min. The temperature of the sample was raised to 773 K at 5 K/min. The sample was held at 773 K for a period of 1 h and then cooled to room temperature in flowing Ar.

(*2*) *Reduction.* The Ar flow was cut off and He was allowed to flow at 300 cm^3/min. The hydrogen flow rate was adjusted to 80 cm^3/min. Since the thermal conductivity of Ar is similar to that of ethane and methane, Ar cannot be used as a carrier gas. The flow rates used during reduction were similar to those used while conducting the reaction. The temperature of the reactor was raised to 773 K at a heating rate of 20 K/min. At

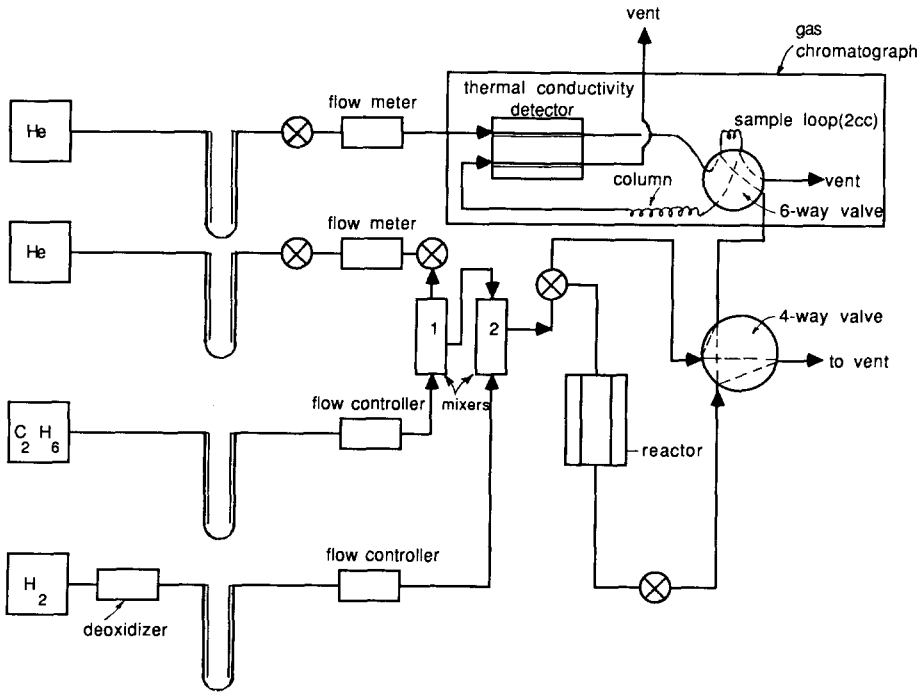

FIG. 1. Schematic diagram of the ethane hydrogenolysis unit.

the end of the reduction process, hydrogen was cut off and the sample was cooled in He to 523 K.

(*3*) *Reaction conditions.* The following gas flow rates were used to conduct the reaction: 300 cm^3/min of He, 80 cm^3/min of H_2, and 20 cm^3/min of C_2H_6. The total flow rate was maintained constant at 400 cm^3/min throughout the study. Thus, the partial pressures of the reactants were kept constant. Since the observed reaction rates could be distorted because of carbon deposition, it is desirable to use as high a $P_{Hydrogen}/P_{Ethane}$ ratio as possible. The partial pressures used in this study are similar to those used by Sinfelt (*26*). Since the activity of each of the catalysts studied was vastly different, the reaction temperature required to maintain differential conditions was found by trial and error. This was achieved by systematically raising the temperature of the reactor from 523 K in steps of 10 K; the reaction was carried out at conversion levels less than 5%. The standard deviation in the activation energies measured was 0.74 kcal/mole.

(*4*) *Sampling.* In a typical experiment, the reactant gases were passed over the catalyst for 3 min prior to sampling. The ethane flow was then cut out and hydrogen and helium flow continued for 15 min prior to another reaction period. This procedure was used to avoid complications due to changing catalyst activity, and it was repeated at each temperature until steady state was achieved. The temperature was varied in a cyclical manner to test for hysteresis effects. Finally, the gas mixture containing ethane, hydrogen, and helium was diverted to bypass the reactor to determine the composition of the feed mixture.

(*5*) *Calibration.* The only product obtained in this reaction is methane. Known amounts of methane and ethane were in-

jected with a gas-tight syringe (Alltech, 25A-RN-GSG Syringe). A linear relationship was observed at low concentration levels. The calibration was periodically verified and was found to be reproducible within 3.5%. Since the thermal conductivity of He and H_2 are similar, the sensitivity of the detector toward H_2 is low. Hence, the GC was not calibrated with respect to hydrogen. The mass balance closure was verified by monitoring the ethane and methane concentrations. Engstrom *et al.* (*18*) have reported the presence of a carbonaceous residue on single-crystal Ir surfaces after ethane hydrogenolysis. In order to test this possibility a catalyst sample that had been subjected to the test reaction was slowly heated (at 3 K/min) in a mixture of helium and hydrogen. The exit gas was periodically sampled and analyzed for methane. No methane was detected. These results suggest that if any carbonaceous residue exists it cannot be removed by heating the used catalyst in hydrogen. Adsorbed carbon, however, may be removed by oxygen (*19*).

RESULTS

Temperature-Programmed Reduction

The TRPd results for the monometal calcined precursors are presented in Table 1. It is seen that the hydrogen consumption observed in the case of Pt precursors is generally lower than those observed in the case of Ir precursors. Quantitative interpretation of hydrogen consumption values are complicated by two factors:

(i) The hydrogen consumption resulting from support reduction is not known (*12, 20*).

(ii) The precise stoichiometry of the precursor after calcination is not known. A study (*20*) on the Pt/Al_2O_3 system indicates the existence of chloride containing surface species of the form $[Pt(OH)_xCl_y]$ and $[PtO_xCl_y]$. Studies conducted on the Ir/Al_2O_3 system (*21, 22*) indicate that the peak in the TPRd spectrum at $\approx$488 K results from the reduction of crystalline IrO_2. Accordingly the *H/M* value for the reduction process should be 4.0. The observed *H/M* ratio is about 2.0. This indicates that only a fraction of the metal complex has been converted to IrO_2; the other fraction has been converted to a lower oxidation state. Previously investigators have employed other experimental techniques to confirm this fact. Xue (*22*) has speculated that the metal species (after calcination) exists in the form of an irreducible core surrounded by IrO_2. Yao *et al.* (*23*) have proposed a similar hypothesis for the Pt/Al_2O_3 system. Hence, the hydrogen consumption cannot be readily related to the oxidation state of the precursor.

The TPRd spectrum for the Ir/Al_2O_3 precursor (Fig. 2) shows the reduction rate maximum at 474 K. This is in agreement with the observations reported by Huang *et al.* (*21*) and Xue (*22*). The observed hydrogen consumption may be related to an "effective" oxidation state according to the following stoichiometry:

$$M^{x+} + H_2 \rightarrow M + (x/2)2H^+ \qquad (2)$$

where M is either Pt or Ir, and x is an "effective" or "average" oxidation state which is also the *H/M* ratio. These quantities are reported in Table 1.

The hydrogen consumption observed for the Al_2O_3-supported precursors are consistently higher than those observed for the TiO_2-supported precursors. Auxiliary X-ray fluorescence experiments showed that the amount of chloride retained by TiO_2-supported precursors after calcination is lower than that retained by the Al_2O_3-supported precursors. This suggests that the amount of hydrogen consumed during reduction may be related to the amount of chlorine present in the precursor after calcination. It is interesting to note that the hydrogen consumption observed for the composite oxide-supported precursors are similar to that observed for the Al_2O_3-supported pre-

TABLE 1

Temperature-Programmed Reduction Results for Pt and Ir Precursors

Quantity	Support							
	Pt precursors				Ir precursors			
	Al_2O_3	TiO_2	0.87% Al_2O_3–TiO_2	11% TiO_2–Al_2O_3	Al_2O_3	TiO_2	0.87% Al_2O_3–TiO_2	11% TiO_2–Al_2O_3
Peak T(K)	380,436	353,373	342,379	393,460	474	460	440,477	483
Total Hz consumed (μmole/g. prec.)	132.5	49.3	103.1	110.8	224.6	39.3	206.6	209.4
TPRd Hz consumption (μmole/g. prec.)	126.4	41.8	99.8	83.8	221.7	36.0	203.8	204.8
Room temp. Hz consumption (μmole/g. prec.)	6.1	7.50	3.3	27.0	2.9	3.3	2.8	4.6
H/M	1.72	0.64	1.34	1.44	2.89	0.51	2.66	2.70

cursors. This observation suggests that the dissolution and readsorption of Al^{3+} originating from Al_2O_3 present in the composite oxide plays a role in altering the reducibility of the precursors. This phenomenon has been explored and the results are presented later.

Temperature-Programmed Desorption

The TPD results, which include the hydrogen emission values and peak temperatures, are presented in Table 2. The first and second TPD spectra for Al_2O_3-supported precursors are identical. The TPD results for the TiO_2-supported precursors indicate that hydrogen chemisorption does not occur when the reduced precursor is cooled in hydrogen presumably because of SMSI (*10, 11*). Likewise, complete suppression in hydrogen chemisorption is also observed in the case of the 11.4% TiO_2–Al_2O_3- and 0.87% Al_2O_3–TiO_2-supported Pt and Ir precursors. Since no hydrogen is chemisorbed during the cooling process, no hydrogen is desorbed during the TPD experiment. The TPD results observed in the present study are in agreement with static chemisorption results reported by McVicker and Ziemiak (*1*). These investigators have shown that the extent of suppression in hydrogen uptake depends upon the relative Group VIII-metal and TiO_2 concentrations on the Al_2O_3 carrier; the higher the TiO_2/Group VIII-metal ratio, the greater the chemisorption suppression.

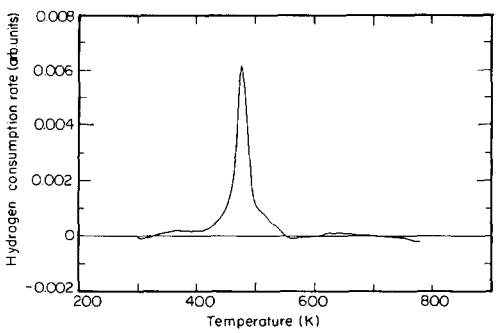

FIG. 2. Temperature-programmed reduction profile for the Ir/Al_2O_3 precursor.

Ethane Hydrogenolysis

Arrhenius plots for the catalysts are shown in Figs. 3 and 4. The activation energy and the preexponential factors were calculated from the slope and intercept of the least-squares fit. The temperature required for achieving a reaction rate of 0.1 g mol of C_2H_6 consumed/(h · g of total metal) has been evaluated. These values are presented in Table 3. Considering the wide vari-

TABLE 2

Temperature-Programmed Desorption Results for Pt and Ir Precursors

Quantity	Support							
	Pt Precursors				Pt Precursors			
	Al_2O_3	TiO_2	0.87% Al_2O_3–TiO_2	11% TiO_2–Al_2O_3	Al_2O_3	TiO_2	0.87% Al_2O_3–TiO_2	11% TiO_2–Al_2O_3
1st TPD H_2 evolved (μmole/g. prec)	40.3	0	0	0	83.4	0	0	0
2nd TPD H_2 Evolved (μmole/g. prec)	40.3	0	0	0	83.4	0	0	0
Peak T(K)[a]	340	—	—	—	363.473	—	—	—

[a] For both first and second TPDs.

ations in materials and preparation variables such as type of procedure, impregnation volume, and activation conditions, the reaction rates reported in the present study are in qualitative agreement with those reported in the literature (*1*, *24–26*).

The effect of variation in dispersion on the ethane hydrogenolysis activity of Rh/TiO_2 catalysts has been studied by Resasco and Haller (*27*). These investigators have shown that the activation energy is almost independent of dispersion; the preexponential, and thus the rate, varies with dispersion. Barbier and Marecot (*28*) have systematically studied the variation in ethane hydrogenolysis activity with the dispersion of Al_2O_3-supported Pt and Ir catalysts. The activity of these catalysts decreases with an increase in dispersion. The study was conducted under isothermal conditions (448 K) and no information on the variation of the activation energy of these catalysts is available. Since Rh belongs to the same family of noble metals, the kinetic behavior of Pt and Ir are assumed to be similar. Therefore, if the apparent activation energy is independent of dispersion, it may be regarded as a function of the metal/support combination. Conversely, if the activation energy is known, this test reaction can be used to distinguish between different metal/support combinations.

The activation energies and preexponential factors for the composite oxide-supported catalysts are different from those reported for the pure oxide-supported

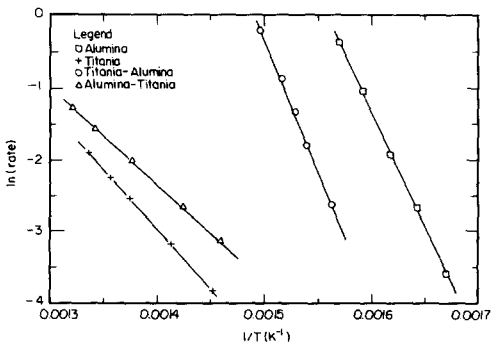

FIG. 3. Arrhenius plots for Pt catalysts. The solid line represents the least-squares fit.

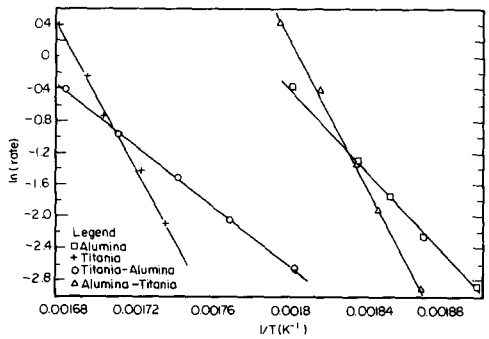

FIG. 4. Arrhenius plots for Ir catalysts. The solid line represents the least-squares fit.

TABLE 3

Activation Energy and Preexponential Factors for I and II Type Catalysts

Catalyst	Type	E (kcal/mol)	ln A	Temp.[a] (K)
Pt/Al_2O_3	I	63.8	49.7	613.4
Pt/TiO_2	I	32.7	19.9	736.4
Pt/11% TiO_2–Al_2O_3	I	74.0	55.2	643.5
Pt/0.87% Al_2O_3–TiO_2	I	27.1	16.6	715.4
Ir/Al_2O_3	I	56.3	50.4	534.1
Ir/TiO_2	I	90.7	76.7	574.0
Ir/11% TiO_2–Al_2O_3	I	38.2	31.8	560.1
Ir/0.87% Al_2O_3–TiO_2	I	93.8	84.7	539.1
Catalyst A	II	58.9	55.3	511.4
Catalyst B	II	62.8	58.0	520.7
Catalyst C	II	89.5	81.7	532.6

[a] Temperature required for rate = 0.1 g mol of ethane consumed/hr/g of metal.

catalysts. The activity of the 0.87% Al_2O_3–TiO_2-supported Ir catalyst is considerably greater than that of the Ir/TiO_2 catalyst. The activity of the 0.87% Al_2O_3–TiO_2-supported Pt catalyst is also greater than that of the Pt/TiO_2 catalyst. The secondary phase in the composite oxide acts as a perturbation and alters the kinetics. It follows from our earlier discussion that the presence of Al_2O_3 leads to readsorption of Al^{3+} during impregnation and the presence of TiO_2 can lead to TiO_x overlayer formation during reduction. Since the potential effects of readsorbed Al^{3+} species (increased hydrogen consumption during TPRd and increased hydrogenolysis activity) are more apparent in the Ir system, these catalysts were chosen for further study.

DISCUSSION

The TPRd and hydrogenolysis results suggest that dissolved/readsorbed Al^{3+} species alter the structure and performance of composite oxide-supported catalysts. Related studies have shown that Ti^{2+} ions are not released into solution because of the strong covalent nature of the Ti–O bond (*36, 37*). In order to investigate the effect of Al^{3+} species, a series of TiO_2-supported Ir precursors and catalysts were prepared in which Al^{3+} in the form of aluminium nitrate was introduced into the chloroiridic acid impregnation solution (Set II). This approach was used to simulate the presence of Al^{3+} species in a system devoid of Al_2O_3. Aluminium nitrate, at the concentration levels used, is completely soluble in the impregnation solution, and it dissociates to Al^{3+} and NO_3^-. All the added Al^{3+} is present in the precursor because it was prepared by dry impregnation. In the case of the 0.87% Al_2O_3–TiO_2-supported Ir precursor, we propose Al_2O_3 dissolves in the acidic impregnation solution, and a fraction of the Al^{3+} ions released into the solution phase is readsorbed. To test this hypothesis, we prepared samples (Set I and Set II types of precursors), where the only difference is in the source of the Al^{3+} ions.

The Al weight loading in the 0.87% Al_2O_3–TiO_2-supported Ir precursor is 0.46%. This corresponds to the maximum amount of aluminum that can be dissolved in the composite oxide system. In reality, the amount of readsorbed aluminum will be less than the total amount of aluminum present as Al_2O_3 in the composite oxide. The amount of Al^{3+} readsorbed is not known precisely. Three types of Set II precursors were prepared. The amount of aluminum nitrate added to the impregnating solution was varied to achieve Al loadings of 0.46%,

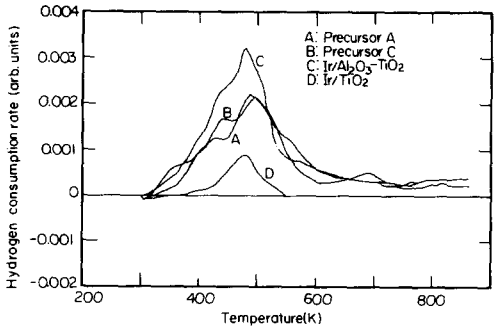

FIG. 5. Temperature-programmed reduction profile for the I and II type precursors.

0.23%, and 0.11%. The precursors were calcined according to the standard procedure. These are referred to as precursors A, B, and C, respectively. Precursor A represents the limiting case corresponding to total dissolution of available Al in the composite oxide (0.87% Al_2O_3–TiO_2) system.

The TPRd profiles for precursors A and C are shown along with those obtained for TiO_2 and 0.87% Al_2O_3–TiO_2-calcined Ir precursors in Fig. 5. The TPRd results are presented in Table 4. It is seen that precursors A and C show a substantial increase in the hydrogen consumption over that observed for the TiO_2-supported precursor. (The TPRd results for precursor B are similar to those obtained for precursors A and C.) The hydrogen consumption observed for precursors A and C are similar to those observed for the 0.87% Al_2O_3–TiO_2-supported precursor; the reduction profiles (peak temperature) are also qualitatively similar. These experiments support the hypothesis that the readsorbed Al^{3+} alters the decomposition of the precursor during calcination and this results in a species that shows a higher hydrogen consumption value.

The hydrogenolysis activity of catalysts A, B, and C was measured. The Arrhenius plots for these data sets as well as Ir supported on Al_2O_3, TiO_2, and 0.87% Al_2O_3–TiO_2 are shown in Fig. 6. The activation energy and the preexponential factor are presented in Table 3. The activity of catalysts A, B, and C is higher than the activity of the Ir/TiO_2 catalyst. The readsorbed Al^{3+} acts like a promoter and increases the activity significantly. Comparing the Pt/TiO_2 and Pt/0.87% Al_2O_3–TiO_2 catalysts, the increase in hydrogen consumption during TPRd as shown in Table 1 and the increase in hydrogenolysis activity as shown in Table 3 indicate that similar trends are observed for Pt catalysts as well.

Figure 7 shows the variation in apparent

TABLE 4

Temperature-Programmed Reduction Results for Type II Precursors

Precursor:	Prec. A	Prec. C	Ir/TiO_2	Ir/0.87% Al_2O_3–TiO_2
Type:	II	II	I	I
Peak T(K)	435,493	344,440,485	460	440,477
Total H_2 consumed (μmole/g. prec.)	222.9	211.0	39.3	206.6
TPRd H_2 consumption (μmole/g. prec.)	222.9	211.0	36.0	203.8
Room temp. H_2 consumption (μmole/g. prec.)	0.0	0.0	3.3	2.8

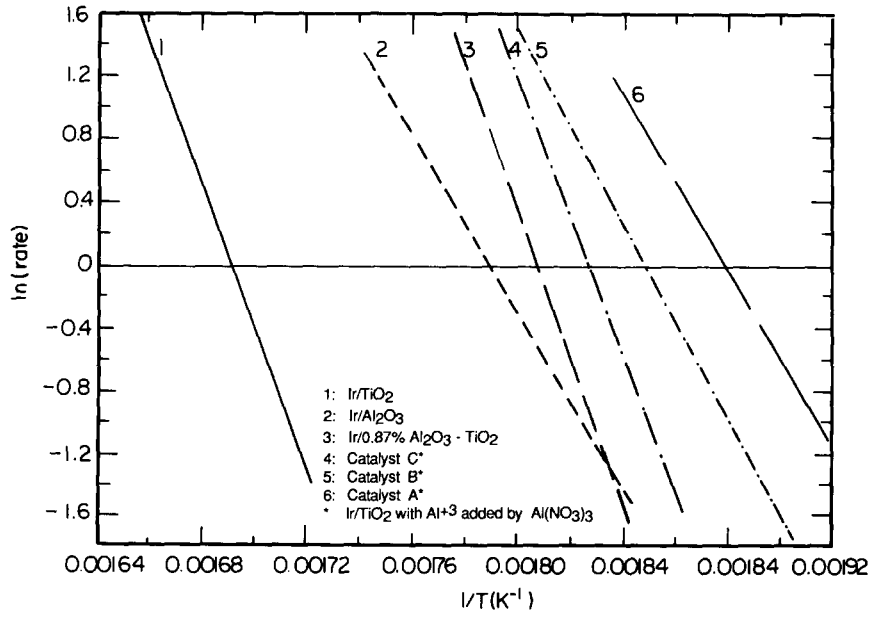

FIG. 6. Arrhenius plots for type II catalysts. The solid line represents the least-squares fit.

activation energy for catalysts A, B, and C. It is interesting to note that there is a direct relationship between the catalytic activity and the amount of Al^{3+} added, and the activity of catalyst C is similar to that of the Ir/0.87% TiO_2–Al_2O_3 catalyst. The activation energy increases with a decrease in the amount of added aluminum. The variation in activation energy could conceivably result from the formation of an Ir–Al entity. The systematic variation in the activities of catalysts A, B, and C suggests that adsorbed Al^{3+} is intimately associated with the noble metal.

Formation of intermetallic compounds or alloys between Al and noble metals like Pt and Ir has been reported in the literature (*29, 30*). Den Otter and Dautzenberg (*29*) have reported the formation of Pt_3Al type of alloys in Pt/Al_2O_3 catalysts when the latter are reduced at around 873 K. Thermodynamic calculations, using bulk properties, indicate Pt–Al alloys to be stable in air at room temperature (*32*). Bronger and Klemm (*33*) have reported that alloys of the form Pt_nAl_m can be prepared by the reduction of a physical mixture of Pt and Al_2O_3 in a stream of ultra-dry H_2. De Bruin *et al.* (*34*) have studied the surface reaction between a Pt film and Al_2O_3 under vacuum at about 1273 K. Sprys and Mencik (*35*) have observed a similar reaction in an electron microscope. Platinum deposited on a thin Al_2O_3 film was seen to consume Al_2O_3 when the Pt film was heated by an intense electron beam. Electron diffraction was used to identify the reaction product as Pt_3Al.

A recent study conducted by Axler and Roof (*30*) indicates that an alloy of the form IrAl can be prepared. These investigators prepared IrAl crystals by pressing metallic Ir into a pellet along with Al_2O_3, Th, Cu, and P. The pellet was allowed to equilibrate at 1423 K for 24 h and then cooled to 933 K at 1 K/h. The IrAl crystals are cubic in nature, and these investigators have shown that IrSi alloys can also be formed. Alloy formation between Al and Ru (Al_2Ru) has also been reported (*31*); these investigators have shown that vapor-deposited Al penetrates the Ru (0001) surface to form the intermetallic compound at 1170 K. Alloys of the

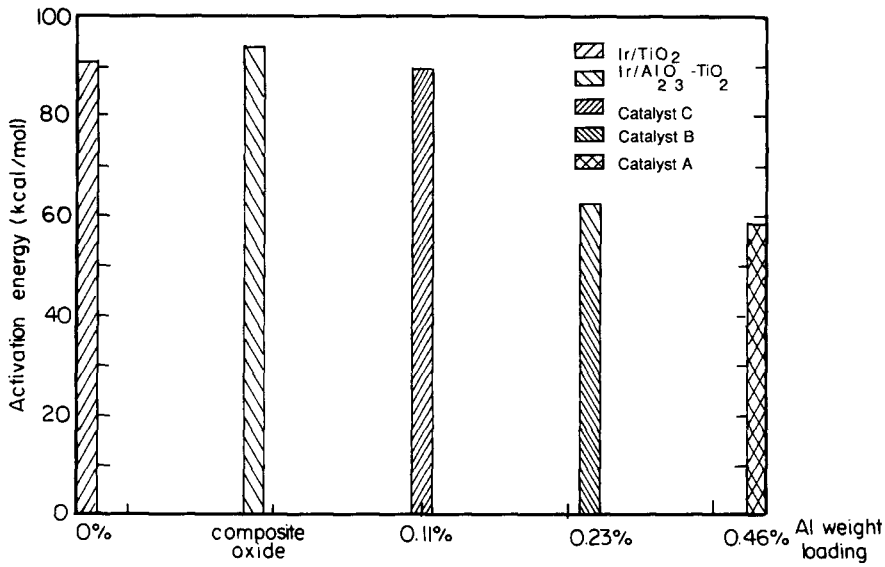

FIG. 7. Variation of activation energy, E, in type II catalysts.

form Pt_xTi_y and Ir_xTi_y are unlikely to be formed because Ti^{2+} ions unlike Al^{3+} ions do not dissolve and readsorb on the surface of the catalyst.

These studies on alloy formation were all conducted on bulk systems and a high temperature was required for alloy formation. The temperature required for alloy formation may be considerably lower in highly dispersed catalysts (*29*). We suggest that IrAl and Pt_2Al type of alloys may exist on the surface when the precursor is reduced to form the working catalyst. The TPRd and ethane hydrogenolysis results reported in this study support the hypothesis that aluminum metal becomes incorporated into the metal matrix and alters the catalytic activity.

The TPRd, TPD, and ethane hydrogenolysis results were used to model the structure of the precursors after calcination and reduction. Ethane hydrogenolysis, a structure-sensitive reaction, provided information on the activity and structure of the catalysts. The TPRd and TPD results were used to assess the reducibility and morphology of the catalysts before and after reduction. The two processes of interest are Al^{3+} dissolution and readsorption and TiO_x overlayer growth. The Al_2O_3 present in the oxide support dissolves in the acidic impregnation solution, and a fraction of dissolved Al^{3+} is readsorbed by the precursor. The Al^{3+} dissolution/readsorption process occurs in Al_2O_3, 11.4% TiO_2–Al_2O_3 and 0.87% Al_2O_3–TiO_2-supported precursors. The extent of decomposition suffered by the precursor during calcination is altered because of the presence of readsorbed Al^{3+}. When the calcined precursors are reduced, three processes occur. The metal present in the higher oxidation state after calcination is reduced to the zero-valent state. Aluminum metal probably gets incorporated into the metal matrix leading to a noble metal–aluminum type of alloy. The incorporation of the readsorbed Al^{3+} increases the activity of these catalysts. The partially reduced TiO_x species, which originates from the TiO_2 present in the support, is mobile in a reducing environment, and the TiO_x species encapsulates the metal. The TiO_2 overlayer formation occurs in the TiO_2, 11.4% TiO_2–Al_2O_3 and 0.87% Al_2O_3–TiO_2-supported precursors. The amount of hydrogen chemisorbed on the catalyst is suppressed

by the physical blockage of the metal surface.

ACKNOWLEDGMENTS

This work was supported by the Department of Energy, Office of Basic Energy Sciences under Grant DE-FG02-87ER-13650. The authors thank Dr. Keith Jones of Brookhaven National Laboratories, Upton, NY, for performing the XRF measurements. The authors also thank Drs. K. Otto and M. S. Chattha of Ford Motor Company for critically reading the manuscript.

REFERENCES

1. McVicker, G. B. and Ziemiak, J. J., *J. Catal.* **95,** 473 (1985).
2. Connell, G., and Dumesic, J. A., *J. Catal.* **101,** 103 (1986).
3. Connell, G., and Dumesic, J. A., *J. Catal.* **102,** 216 (1986).
4. Connell, G., and Dumesic, J. A., *J. Catal.* **105,** 285 (1987).
5. Jin, T., Hattori, H., and Tanabe, K., *Bull. Chem. Soc. Japan* **55,** 2279 (1982).
6. Santacesaria, E., Gelosa, D., and Carra, S., *Ind. Eng. Chem. Prod. Res. Dev.* **16,** 45 (1977).
7. Sacconi, L., *Discuss. Faraday Soc.* **7,** 173 (1949).
8. Maatman, R. W., Mahatty, P., Hoekstra, P., and Addink, C., *J. Catal.* **23,** 105 (1971).
9. Mieth, J. A., Huang, Y. J., and Schwarz, J. A., *J. Colloid Interface Sci.* **1123,** 374 (1988).
10. Tauster, S. J., Fung, S. C., and Garten, R. L., *J. Amer. Chem. Soc.* **100,** 170 (1978).
11. Tauster, S. J., and Fung, S. C., *J. Catal.* **55,** 29 (1978).
12. Baker, R. T. K., Tauster, S. J., and Dumesic, J. A., Eds., "Strong Metal-Support Interactions." ACS Symposium Series 298, Washington, DC, 1986.
13. Nobile, A., Jr., and Davis, M. W., *J. Catal.* **116,** 383 (1989).
14. Vannice, M. A., and Garten, R. L., *J. Catal.* **56,** 236 (1979).
15. Vannice, M. A., Twu, C. C., and Moon, S. H., *J. Catal.* **79,** 70 (1983).
16. Subramanian, S., Noh, J. S., and Schwarz, J. A., *J. Catal.* **114,** 433 (1988).
17. Huang, Y.-J., Xue, J., and Schwarz, J. A., *J. Catal.* **111,** 59 (1988).
18. Engstrom, J. R., Goodman, D. W., and Weinberg, W. H., *J. Amer. Chem. Soc.* **110,** 8305 (1988).
19. Fung, S. C., private communication, 1989.
20. Lieske, H., Lietz, G., Spindler, H., and Völter, J., *J. Catal.* **81,** 8 (1983).
21. Huang, Y.-J., Fung, S. C., Gates, W. E., and McVicker, G. B., *J. Catal.*, **118,** 192 (1989).
22. Xue, J., "The Study of Ir/Al_2O_3, Pt/Al_2O_3 and $Pt–Ir/Al_2O_3$ Catalysts," M.S. thesis, Syracuse University, New York, 1987.
23. Yao, H. C., Sieg, M., and Plummer, H. K., Jr., *J. Catal.* **59,** 365 (1979).
24. Foger, K., and Anderson, J. R., *J. Catal.* **59,** 325 (1979).
25. Ko, E. I., and Garten, R. L., *J. Catal.* **68,** 233 (1981).
26. Sinfelt, J. H., *J. Phys. Chem.* **68,** 344 (1964).
27. Resasco, D. E., and Haller, G. L., *Stud. Surf. Sci. Catal.* **11,** 105 (1982).
28. Barbier, J. and Marecot, P., *Nouv. J. Chim.* **5,** 393 (1981).
29. Den Otter, G. J., and Dautzenberg, F. M., *J. Catal.* **53,** 116 (1978).
30. Axler, K. M., and Roof, R. B., *Adv. X-Ray Anal.* **29,** 333 (1986).
31. Campbell, C. T., and Goodman, D. W., *J. Phys. Chem.* **92,** 2569 (1988).
32. Klemm, W., Dorn, F., and Huch, R., *Naturwissenschaften* **45,** 490 (1958).
33. Bronger, W., and Klemm, W., *Z. Anorg. Allgem. Chem.* **58,** 319 (1962).
34. De Bruin, H. J., Moodie, A. F., and Warble, C. E., *J. Mater. Sci.* **7,** 909 (1972).
35. Sprys, J. W., and Mencik, Z., *J. Catal.* **40,** 290 (1975).
36. Subramanian, S., Ph.D dissertation, Syracuse University, Syracuse, NY.
37. Grant, R., *Rev. Mod. Phys.* **31,** 646 (1959).